The load-bearing capacity of Steel-HPC composite beams

Autor(en): **Bullo, Sandra / Di Marco, Roberto**

Objekttyp: **Article**

Zeitschrift: **IABSE reports = Rapports AIPC = IVBH Berichte**

Band (Jahr): **999 (1997)**

PDF erstellt am: **08.08.2024**

Persistenter Link: https://doi.org/10.5169/seals-961

The Load-Bearing Capacity of Steel-HPC Composite Beams

Sandra BULLO
Architect
Univ. Inst. of Arch.
Venice, Italy

Sandra Bullo, born in 1963, graduated in architecture in Venice, subsequently specialising in R.C. structures at the Milan Polytechnic. Her main research interests are in steel-concrete composite structures and in creep effects in non-homogeneous structures.

Roberto DI MARCO
Associate Professor
Univ. Inst. of Arch.
Venice, Italy

Roberto Di Marco, born 1948, is Associate Professor of Civil Engineering. At present he is carrying out research on non-linear analysis of R.C. structures, on the use of new materials in civil engineering.

Summary

As far as steel-concrete composite beams are concerned, the use of high performance concrete (HPC) gives rise to an increased stiffness in the shear connectors and a reduction in ultimate slipping.
A numerical simulation referring to simply supported beams demonstrates that, at least in the case of full interaction, the brittle behaviour of the connection does not significantly affect the load-bearing capacity of the structure because flexural failure of the midspan section due to rupture of the materials occurs before any shear failure of the connection due to its capacity for deformation being exceeded.

1. Introduction

The mechanical characteristics of high performance concrete (HPC) lead to a variation in the behaviour of the beam-slab system, relating to two distinct factors:
- a variation in the behaviour of the cross section because of the greater strength and stiffness of the concrete forming the slab;
- a marked change in the behaviour of the shear connectors between the two elements.

Experimental tests on stud connectors, forming part of a research program being developed at the University Institute of Architecture in Venice, have shown that, as the strength of the concrete increases, there is an increase in both the strength and the stiffness of the connection, while there is a significant reduction in its ductility /1/.
It is therefore essential to investigate the effects that the brittle behaviour of the connector may have on the behaviour of the beams - be it in the case of a full connection or of a partial connection - because if the slip requirement is greater than the slip capacity of the connectors, then shear failure will occur before the ultimate flexural load is reached.
A parametric investigation was developed, varying both the mechanical characteristics of the materials and the geometric dimensions of the cross sections, to assess ductility requirements in different conditions and identify any design rules.

2. Effects of the concrete's strength on the behaviour of the connector

Fig. 1 and Table 1 illustrate some of the results of the experimental trials that the authors performed on the behaviour of stud connectors by means of push-out tests on standard samples. Said results show that a higher-strength concrete coincides with an increase in strength and stiffness, but also with a reduction in the extent of slipping at failure (s_c) and at the maximum load (s_u).

R_{cm} (MPa)	P_{max} (kN)	s_u (mm)	s_c (mm)
32.50	109.16	5.597	7.865 (*)
59.55	153.00	4.398	6.023 (*)
94.40	191.82	3.538	3.740

((*) slipping measured when P has fallen to $0.95 \cdot P_{max}$)

Table 1 Average experimental values for maximum loads and slipping of Nelson connectors (R_{cm}=mean cubic compressive strength, shank diameter ϕ=19 mm).

3. Numerical Model

The study assessed the load-bearing capacity of simply supported composite beams, with uniformly distributed load, considering both the behaviour of the HPC and the load-slip relationships that can reproduce the behaviour of shear connectors in HPC.
Since the problem is far from linear, an incremental procedure till the collapse was used: at each step, the solution was found using an iterative process on the cross sections discretized in strips and along the axis of the beam divided into short lengths dx.
The model assumed the linearity of the strains in the steel beam and slab cross sections (indexes s and c,respectively) (Fig. 1) and any effects of the lifting of the slab were disregarded in view of their scarce influence on the slipping value emerging from the study /2/.
Having assumed the sectional deformations (the strain $\varepsilon_{os}(x)$ of the top fiber of the steel part; the curvature $\chi(x)$ common to the two elements; and the relative slipping s(x)) as unknown quantities, the conditions of equilibrium were established. In view of the presence of slipping, the equilibrium condition for the shear stresses at the beam-slab interface was added to the usual equilibrium conditions for the translation and rotation of the section.

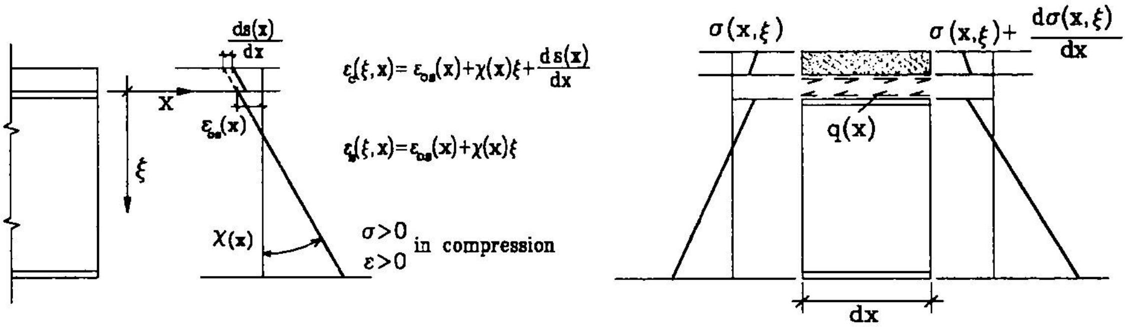

Fig. 1 Deformation in the section and beam length dx.

Taking a secant linear formulation for the constitutive laws into account, the system for finding the solution took shape as follows:

$$\varepsilon_{os}(x)[EA]+\chi(x)[ES]+\frac{ds(x)}{dx}[EA]_c=0$$

$$\varepsilon_{os}(x)[ES]+\chi(x)[EI]+\frac{ds(x)}{dx}[ES]_c=-M(x) \qquad (1)$$

$$\frac{d\varepsilon_{os}(x)}{dx}[EA]_s+\frac{d\chi(x)}{dx}[ES]_s=-q(x)$$

where:

- [EA], [ES], [EI], $[EA]_c$, $[ES]_c$ are the stiffness coefficients of the whole section and of the slab, depending on the state of deformation across the secant modulus of the materials $E_{c,sec}$ and $E_{s,sec}$;

- $\overline{[EA]}_s$, $\overline{[ES]}_s$ are the stiffness coefficients of the steel section, depending on the variation in the deformation in dx, across the secant modulus relating to said variation ($\overline{E}_{s,sec} = d\sigma/d\varepsilon$);

- q(x) is the shear action per unit of length coming to bear on the connector ($q(x)=R_{sec}\, s(x)$; R_{sec} is the secant stiffness of the connector per unit of length).

The finite differences method was used, applying backward integration, to solve the differential equations comprising system (1).
Once the boundary conditions had been established ($\varepsilon_{os}(x=0)=0$; $\chi(x=0)=0$; $s(x=L/2)=0$), the solution was obtained by applying the shooting technique, i.e. having assigned an arbitrary value to s(x=0), system (1) was then solved for the subsequent sections up to the midspan. The procedure was iterated, updating s(x=0), until the condition s(x=L/2)=0 was satisfied.

4. Numerical analysis

The analysis was performed in order to emphasize the extent of the maximum slip requirement in relation to changes in the following parameters:
- the reaction of the connector and slab to changes in the strength of the concrete;
- the span of the composite beam;
- the arrangement of the connectors along the beam.

4.1. Properties of the materials

The following constitutive laws were used:
- for the steel: elasto-plastic strain-hardening law, with the strain-hardening amounting to 100 MPa;
- for the concrete: the non-linear laws proposed in the Model Code 1990 with crushing strain $\varepsilon_{cu}= 0.0038$ and, in the case of HPC, in the Recommended Extension to the Model Code /3/, with crushing strain $\varepsilon_{cu}= 0.0030$.

4.2. Properties and arrangement of the connectors

The load-slip law of the connector was modeled by means of the exponential relationship proposed by Ollgaard /4/, and already used in /2/, /5/, /6/, /7/, /8/:
$P=P_u(1-e^{-\beta s})^\alpha$

where: $\alpha=1.7$, $\beta=1.15$ mm^{-1}, $s_c=7.0$ mm for the type 1 curves (studs in ordinary concrete)
$\alpha=0.5$, $\beta=1.10$ mm^{-1}, $s_c=3.5$ mm for the type 1 curves (studs in HPC) (Fig. 2)

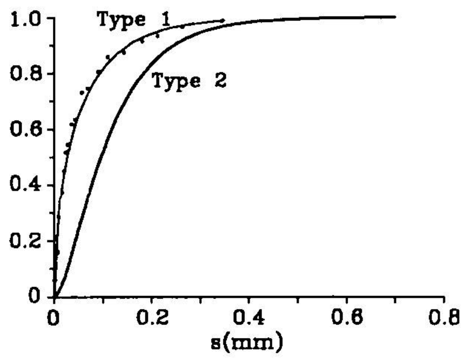

Fig. 2 Load-slipping relationships

having obtained the values of the coefficients α e β from an analysis of the results reported in the literature (for the type 1 curve) /9/ or from a fitting operation on experimental findings obtained by the authors (for the type 2 curve) /1/.
Two solutions were considered for the distribution of the connectors along the beam:
- evenly distributed (arrangement type A);
- evenly distributed at intervals, following the distribution of the shear stresses under a constant load (arrangement type B).

4.3. Numerical tests

The investigation considered beams characterized by the cross sections illustrated in Fig. 3, with spans of 15, 25, 30 and 40 m, mean cylindrical concrete strengths of 35 and 80 MPa, and connectors having the constitutive laws of Fig. 2, according to the following table.

CODE	NC1-15	NC2-15	NC1-25	HP2-15	HP2-25	NC1-30	NC1-40	HP2-30	HP2-40
f_{cm} (MPa)	35	35	35	80	80	35	35	80	80
P-s	Type 1	Type 2	Type 1	Type 2	Type 2	Type 1	Type 1	Type 2	Type 2
Span L (m)	15	15	25	15	25	30	40	30	40
L/H	13.0	13.0	21.5	13.0	21.5	13.3	17.8	13.3	17.8

Table 2 Characteristics of beams for numerical tests

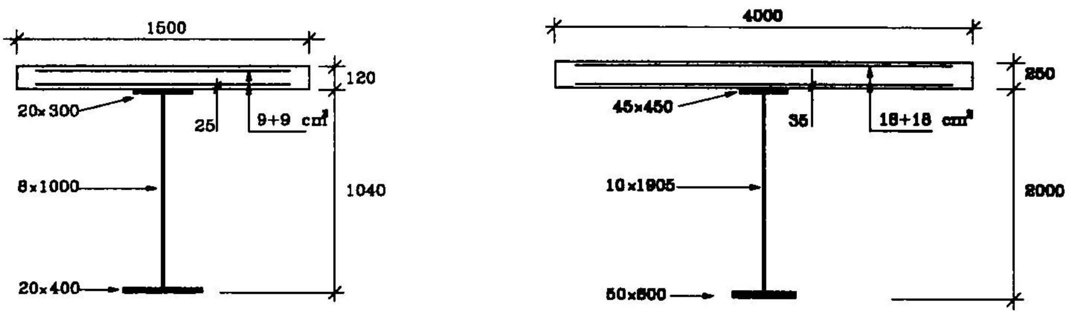

Fig. 3 Cross sections of beams for numerical tests

The maximum global strength of the connectors (Q_d) for the creation of the full shear connection was established by means of an elasto-plastic analysis of the cross section with no slipping.

4.4. Numerical test results

For each of the cases considered, the most significant results are given in Table 3.

CODE	NC1-15	NC2-15	NC1-25	HP2-15	HP2-25	NC1-30	NC1-40	HP2-30	HP2-40
$M_{max,sez}$ (kN*m)	4830.8	4830.8	4830.8	5113.3	5113.3	30225.0	30225.0	31645.0	31645.0
$M_{max}/M_{max,sez}$	0.9933	0.9957	0.995	0.986	0.987	0.987	0.989	0.991	0.988
$slip_{max}$ (mm)	3.275	2.583	4.095	1.651	1.841	3.196	3.367	2.563	2.717
$slip_{max}/s_u$	0.468	0.738	0.585	0.470	0.525	0.457	0.481	0.732	0.776

Table 3 Numerical test results

These data show that, assuming a perfect interaction between the two materials ($\varepsilon_c=\varepsilon_s$), the load-bearing capacity of the beam (M_{max}) is always lower than might be expected on the basis of the flexural strength of its midspan cross section ($M_{max,sez}$).
In fact, the increase in the load applied, and consequently in the acting moment, coincides with an increase in the rate of slipping $ds/dx=\varepsilon_c-\varepsilon_s$ (curves a and b, Fig. 5, for the two types of concrete) and this leads to a reduction in the values of both the maximum resisting moment and the ultimate moment (curves c and d for the ordinary concretes, and f and g for the HPC, Fig. 5). The maximum load that the beam can withstand is the load at which the acting moment at the midspan cross section reaches the same value as the resisting moment, with the corresponding value of the parameter ds/dx; further loading is impossible because it would induce a corresponding increment in the acting moment and in ds/dx, and hence a reduction in the resisting moment.

New equilibrium conditions beyond the maximum load condition can only be achieved by reducing the actions, and the branch of the loading curve up to failure due to the maximum strength threshold being reached becomes unstable.

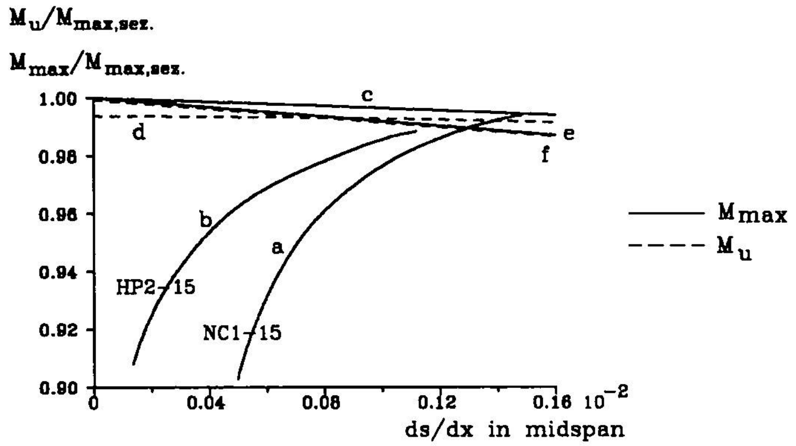

Fig. 4 M_{max} and M_u with changing values of ds/dx

The reduction in resisting capacity with ds/dx becomes more obvious in the case of HPC slabs. Moreover, the greater stiffness of the slab and connection - due to the higher strength of the concrete - gives rise to a reduction in the maximum slipping at failure, so the reduction in load-bearing capacity remains proportionally almost independent of the type of concrete, and the ductility of the connectors (though lower than in the case of ordinary concretes) is sufficient to prevent brittle failure of the beam due to rupture at the connection (Table 3 compares the findings for NC1-15, NC2-15, HP2-15).

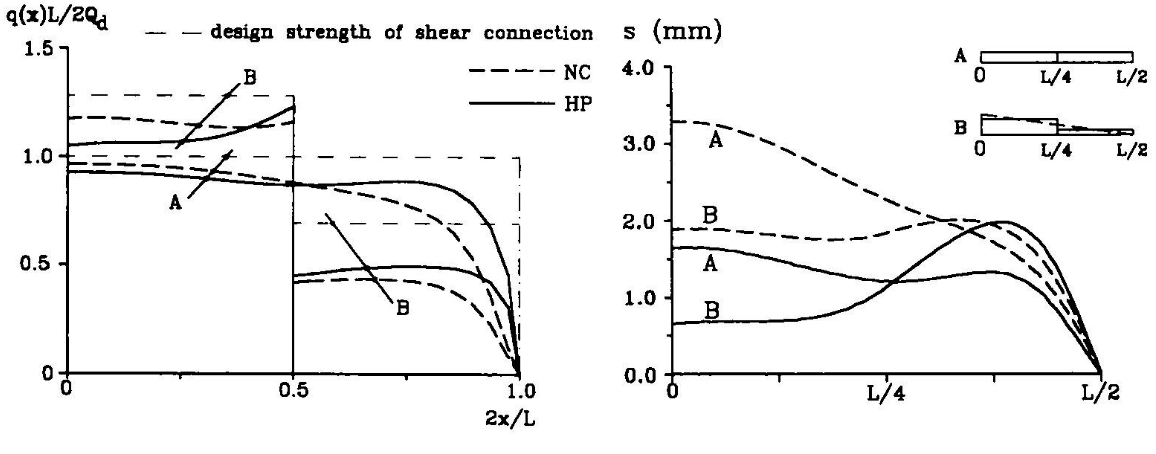

Fig. 5 Shear stresses and slipping along the connection for beams NC1-15 and HP2-15, and for stud connector arrangements A and B.

Fig. 5 shows the distributions of the theoretical resisting actions of the connector (which are uniform in case A, whereas they are twice as great in the supporting area as in the middle of the beam in case B) and the distributions of the actual stud reactions when the maximum load-bearing capacity is reached.
From a comparison of the diagrams, it is clear that the design conditions, based on the assumption f a full plasticization of the connector, coincide substantially with the actual situation in both types of concrete.

The beam-stud-slab system therefore seems, even in the case of HPC, to allow for a redistribution of the stresses, having a generally ductile behavior instead of the brittle behavior detected in the connector alone.
The two distributions consequently prove virtually equivalent in terms of load-bearing capacity, but the same cannot be said for the slipping requirement. The diagram in Fig. 5 shows that, in the case of ordinary concrete, the type B arrangement of the connectors leads to a more uniform distribution of slipping than with the type A arrangement, also reducing the maximum slipping value; in the case of HPC, on the other hand, the uneven distribution of the slipping phenomena is accentuated and their maximum value, which is reached nearly the middle of the beam, is greater than in the case of the uniform (type A) connector arrangement.

6. Conclusions

This study has shows that the behaviour at failure of composite beams made with HPC is influenced not only by changes in the behaviour of the connection, but also by the interaction of the latter with the resistant and deformative reaction of the slab.
In the cases considered here, the ultimate load coincided with flexural failure, thanks also to the contribution of the HPC slab towards reducing the slip requirement.
The study has also demonstrated that the arrangement of the connection is of little significance for the purposes of flexural failure, whereas the arrangements considered were far from comparable in terms of any failure occurring due to the ultimate slipping threshold being exceeded, so special attention must be paid to the identification of the ideal arrangement of the connectors.

References

1. S. BULLO, R. DI MARCO: "Effects of high-performance concrete on stud shear connector behavior", Proceedings of Nordic Steel Construction Conference, Malmö, Sweden, June 1995, pp. 577-584.
2. J. M. ARIBERT, K. ABDEL AZIZ: "Calcul des poutres mixtes jusqu'à l'état ultime avec un effect de soulèvement à l'interface acier-béton", Construction Métallique, n°. 4, 1985, pp.3-36.
3. CEB: Bulletin d'Information n. 228 "High performance concrete - Recommended extensions to the Model Code 90", July 1995.
4. J. G. OLLGAARD, R. G. SLUTTER, J. W. FISHER: "Shear strength of stud connectors in lightweight and normal-density concrete", Engrg. J. Am. Inst. Steel Constr., vol. 8, April 1971, pp. 55-64.
5. J. M. ARIBERT, A. G. LABIB: "Modèle de calcul élasto-plastique de poutres mixtes à connexion partielle", Construction Métallique n°. 4, 1982, pp. 3-51.
6. J. M. ARIBERT: "Etude critique par voie numérique de la méthode proposée dans l'Eurocode 4 pour le dimensionnement des poutres mixtes acier-béton à connexion partielle", Construction Métallique, n.1, 1988, pp. 3-26.
7. R. P. JOHNSON, N. MOLENSTRA: "Partial shear connection in composite beams for buildings", Proc. Instn. Civ. Engrs., Part 2, vol. 91, Dec. 1991, pp. 679-704.
8. S. BULLO, R. DI MARCO: "Influenza della limitata capacità di scorrimento della connessione sulla portanza di travi miste realizzate con calcestruzzi ad alte prestazioni", C.T.E., Napoli, 7-9 November 1996, pp. 21-30.
9. D. J. OEHLERS, C. G. COUGHLAN: "The shear stiffness of stud shear connectors in composite beams", Journal of Construct. Steel Research, n.6, 1986, pp.273-284.
10. D. J. OEHLERS, G. SVED: "Composite beams with limited-slip-capacity shear connectors", Journal of Structural Engineering, Vol. 121, No. 6, June 1995, pp. 932-938.
11. EUROCODE N.4: "Design of composite steel and concrete structures", Part 1-1: General rules and rules for buildings, ENV 1994-1-1, October 1992.